Journal of Alloys and Compounds 753 (2018) 329–332

Contents lists available at ScienceDirect

Journal of Alloys and Compounds

journal homepage: http://www.elsevier.com/locate/jalcom

Giant exchange bias effect with low-coercivity in $YbBaCo_4O_7$

K. Dey [a, b], S. Majumdar [a], S. Giri [a, *]

[a] Department of Solid State Physics, Indian Association for the Cultivation of Science, Jadavpur, Kolkata, 700032, India
[b] S.B.S.S. Mahavidyalaya, Goaltore, 721128, India

ARTICLE INFO

Article history:
Received 31 January 2018
Received in revised form
13 April 2018
Accepted 18 April 2018
Available online 21 April 2018

Keywords:
Geometric frustration
Kagomé lattice
Antiferromagnetic ordering
Exchange bias effect

ABSTRACT

We observe significant exchange-bias effect below ~ 76 K in antiferromagnetic $YbBaCo_4O_7$. Exchange-bias field (H_E) is ~ 10 kOe for 50 kOe cooling-field (H_{cool}) at 4 K. The H_E increases considerably with H_{cool} associated with the nominal increase of coercivity (H_C). Low H_C provides high value of H_E/H_C (~ 15) at 4 K. High H_E/H_C ratio and nominal increase of H_C are appealing. The results suggest robust EB effect associated with the minimal occurrence of inhomogeneous micro-domains, which is potential for the applications. Magnetic phase separation between antiferromagnetic components with $\mathbf{k}_1 = (0, 0, 0)$ and $\mathbf{k}_2 = (1/2, 0, 0)$ propagation vectors of the $Pbn2_1$ space group is correlated with the exchange-bias effect.

1. Introduction

The exchange bias (EB) effect is a six decade old phenomenon which was first observed in the Co/CoO nanoparticles having coreshell structure [1]. The conventional EB effect is manifested through the shift in the magnetic hysteresis loop when the material is cooled through the Néel temperature in a static magnetic field for a combination of ferromagnetic (FM) and antiferromagnetic (AFM) substances [1–8]. After the discovery of EB in a classic combination of FM/AFM substances, this has also been explored in diverse combinations of magnetic substances, which creates intricacy for understanding the EB phenomenon. In the last decade EB effect has also been observed in the chemically single phase alloys and compounds [9]. Despite of the extensive studies of EB effect in plenty of systems, the origin of loop shift is not yet completely understood because of complex interface mechanism. Nevertheless, observation of EB effect is important for the fundamental interests, because it confirms microscopic magnetic phase separation in a chemically single phase compound, which can be simply probed from the bulk magnetization studies [10–12]. The EB effect is also significant for the technological applications such as data storage products, spintronic devices, permanent magnets [2–4,13].

The compound of our interest belongs to the 114-type rare earth (R) cobaltite family with formula $RBaCo_4O_7$. The $RBaCo_4O_7$ attracts special attention for the geometric magnetic frustration, where Co ions residing in CoO_4 tetrahedra form an alternate stacking layers of Kagomé and triangular lattices along the crystallographic c axis [14]. The compound $YbBaCo_4O_7$ revealed a first-order transition to an orthorhombic structure with $Pbn2_1$ space group from the trigonal $P31c$ space group around 175 K [15]. It has been suggested that the significant number of under-bonded Ba^{2+} site in the high temperature phase gave rise to the structural transition around 175 K. This structural instability was found to be associated with the strong softening of Young modulus [16]. Significant oxygen storage capacity has been tested for $YbBaCo_4O_7$ [17]. The effects of Pb doping on the thermoelectric properties were investigated for $Yb_{1-x}Pb_xBaCo_4O_7$, where the Pb doping led to the decrease of electrical resistivity as well as Seebeck coefficient [18]. The neutron diffraction studies have been performed on $YbBaCo_4O_7$, proposing that, the symmetry lowering attributed to the structural transition around 175 K led to the release of geometric magnetic frustration. As a result of it, an AFM long range ordering developed below 76 K with two propagation vectors, $\mathbf{k}_1 = (0, 0, 0)$ and $\mathbf{k}_2 = (1/2, 0, 0)$ of the $Pbn2_1$ space group [15]. The $\mathbf{k}_1 = (0, 0, 0)$ propagation vector has also been observed for isostructural $YBaCo_4O_7$ [19]. Thus $\mathbf{k}_2 = (1/2, 0, 0)$ propagation vector was suggested from a contribution of rare earth moment, although the complete magnetic structure is yet to be determined.

In order to probe the nature of magnetic ordering, further magnetization studies are performed. Our careful observation reveals the evident signature of giant EB effects in $YbBaCo_4O_7$. The value of EB field (H_E) is ~ 10 kOe for 50 kOe cooling field (H_{cool}). The

* Corresponding author.
E-mail address: sspsg2@iacs.res.in (S. Giri).

https://doi.org/10.1016/j.jallcom.2018.04.205
0925-8388/

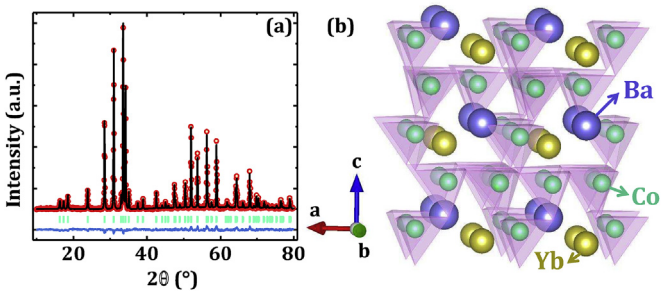

Fig. 1. (a) Rietveld refinement of x-ray powder diffraction patterns (red symbols) at 300 K, (b) atomic arrangements fitted in a *P*31*c* space group. (For interpretation of the references to colour in this figure legend, the reader is referred to the Web version of this article.)

large H_E without any doping is unique [20]. Large value of H_E/H_C ratio ($\sim$ 15) is observed. High H_E/H_C ratio associated with the small value of H_C in $YbBaCo_4O_7$ is unique and indicates that the unidirectional anisotropy involves minimal occurrence of inhomogeneous micro-domains due to field cooling process. Unlike usual consequences, the comparatively homogeneous domains and interfaces involving EB effect are attractive for searching potential spintronic materials. As proposed by the neutron results the magnetic phases involving antiferromagnetic $\mathbf{k}_1 = (0, 0, 0)$ and $\mathbf{k}_2 = (1/2, 0, 0)$ propagation vectors are suggested to be engaged with the observed EB effect.

2. Experimental details

The polycrystalline compound $YbBaCo_4O_7$ is prepared using solid state reaction by mixing stoichiometric ratios of the Yb_2O_3, $BaCO_3$ and Co_3O_4 [21]. Transmission electron microscopy (TEM) is carried out by using a JEOL TEM, 2010 microscope. The crystalline phase is identified by the powder x-ray diffraction patterns (XRD) using a BRUKER axs (Model: 8D - ADVANCE) diffractometer with a CuK_α radiation source. The magnetization (M) is measured using a commercial superconducting magnetometer of UK Cryogenics. Thermal variation of resistivity is recorded using a commercial physical property measurement system (PPMS-II) of Quantum Design.

3. Experimental results and discussions

Fig. 1(a) depicts the x-ray powder diffraction pattern at 300 K. Rietveld refinement is done using *P*31*c* space group. The refined pattern is shown by the continuous curve. The Rietveld fitting seems to be quite satisfactory as revealed by the blue difference plot and the small values of the parameters, R_w (%) (4.06), R_{wp} (%) (2.12), and σ (1.91). The values of refined lattice parameters are $a = 6.2693(2)$ and $c = 10.2310(3)$ [14,15]. As obtained from the refinement the Co ions residing at the CoO_4 tetrahedra associated with other atoms are depicted in Fig. 1(b). In Fig. 2(a) high resolution TEM image shows the lattice fringes. We note that the planes extend up to the edge of the particle. The value of interplanar spacing is $\sim 5.45\,\AA$, which corresponds to the (100) plane, as also confirmed from the x-ray diffraction pattern. The results of the element mapping of Co, Yb, and Ba are displayed in Fig. 2(c–e), respectively for a selected area of the sample as also displayed in Fig. 2(b). The homogeneous distribution of the elements confirms homogeneity of the chemical phase.

Temperature (T) variation of zero-field cooled (ZFC) and field-cooled (FC) magnetization curves measured with a 20 kOe magnetic field are depicted in Fig. 3(a). The ZFC curve deviates from the FC curve around $\sim$ 76 K (T_N), at which a long range antiferromagnetic (AFM) order was confirmed from the neutron diffraction study [15,21]. A step-like feature is observed below $\sim$ 180 K in $M(T)$, which is highlighted in Fig. 3(b). The evident signature of thermal hysteresis is consistent with the first order transition [15]. Thermal hysteresis associated with the similar step-like feature is also observed below $\sim$ 180 K in the resistivity [$\rho(T)$] recorded in zero-field, as depicted in Fig. 3(c). The evident signatures point to the structural coupling to the $M(T)$ and $\rho(T)$. These results are significant, because these structural signatures confirm the O_7 oxygen stoichiometry in $YbBaCo_4O_7$ [21]. Inverse of the susceptibility (χ^{-1}) is depicted with temperature in the inset of Fig. 3(a). The straight line exhibits the Curie-Weiss fit with paramagnetic moment (μ_{eff}) and Curie-Weiss temperature to be 7.0 μ_B/formula unit and -305 K, respectively. The experimentally obtained μ_{eff} value is below the full moment value considering the high-spin moment of Yb^{3+} and Co^{2+}. The results are consistent with that proposed coexistence of major Co^{2+} and minor Co^{3+} ions in $YbBaCo_4O_7$ [21]. We note that the value of θ/T_N is $\sim$ 3.8, proposing considerable magnetic frustration. This is consistent with the coexistence of magnetically frustrated kagomé and triangular lattice arrangements formed by the AFM Co ions.

A non-linear magnetic hysteresis loop with coercivity (H_C) of $\sim$ 505 Oe is observed at 4 K, which does not show any saturating trend at 80 kOe. When the sample is cooled in a static magnetic field from 300 K, the considerable shift of the magnetic hysteresis is observed at 4 K. The shift is positive for negative H_{cool} and negative for positive H_{cool}, which is a typical manifestation of the conventional EB effect. An example of both the positive and negative shifts at 4 K is depicted in Fig. 4(a) for $H_{cool} = \pm 10$ kOe. Central portions of the loops are further highlighted in Fig. 4(b). From the shift of the

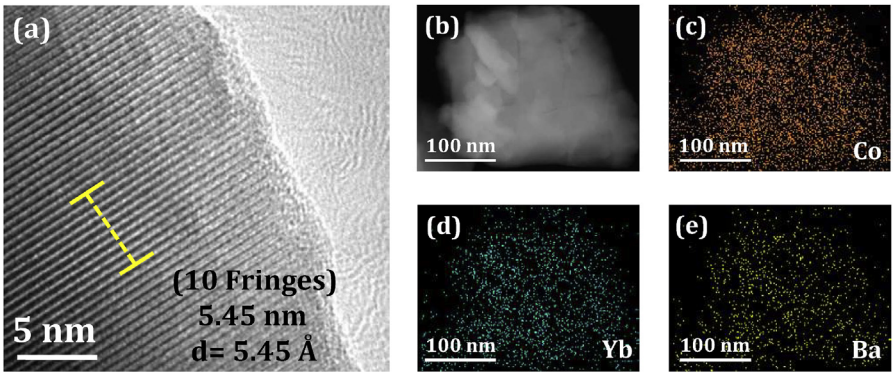

Fig. 2. (a) High resolution TEM image, element mapping analysis of (b) a portion of sample, for (c) Co, (d) Yb, (e) Ba.